# Quantitation of Fluorescence Energy Transfer Between Cell Surface Proteins via Fluorescence Donor Photobleaching Kinetics

Russell M. Young, J. Kenneth Arnette, Deborah A. Roess, and B. George Barisas

Departments of Chemistry and Physiology, Colorado State University, Fort Collins, Colorado 80523 USA

ABSTRACT    We describe practical aspects of photobleaching fluorescence energy transfer measurements on individual living cells. The method introduced by T. M. Jovin and co-workers (see, most recently, Kubitscheck et al. 1993. *Biophys. J.* 64:110) is based on the reduced rate of irreversible photobleaching of donor fluorophores when acceptor fluorophores are present. Measuring differences in donor photobleaching rates on cells labeled with donor only (fluorescein isothiocyanate-conjugated proteins) and with both donor and acceptor (tetramethylrhodamine-conjugated proteins) allows calculation of the fluorescence energy transfer efficiency. We assess possible methods of data analysis in light of the underlying processes of photobleaching and energy transfer and suggest optimum strategies for this purpose. Single murine B lymphocytes binding various ratios of donor and acceptor conjugates of tetravalent concanavalin A (Con A) and divalent succinyl Con A were examined for interlectin energy transfer by these methods. For Con A, a maximum transfer efficiency of 0.49 ± 0.02 was observed. Under similar conditions flow cytometric measurements of donor quenching yielded a value of 0.54 ± 0.03. For succinyl Con A, the maximum transfer efficiency was 0.36. To provide concrete examples of quantities arising in such energy transfer determinations, we present examples of individual cell data and kinetic analyses, population rate constant distributions, and error estimates for the various quantities involved.

## INTRODUCTION

Many problems in biophysics and biochemistry involve assessing the proximities of intra- and intermolecular sites. Such problems include the organization of cell membrane components, antigen-antibody interactions, and relative positions of functional groups within protein and DNA molecules. While distances on the order of micrometers or larger can be measured with techniques such as microscopy, only fluorescence energy transfer (FET) reflects separations on the Ångstrom distance scale. FET measurements have been reviewed by Stryer (1978) and Fairclough and Cantor (1978).

A variety of methods have been used to implement FET for biophysical applications. The most common among these are steady-state techniques including fluorescence spectroscopy (Fleming et al., 1979; Fung and Stryer, 1978; Fernandez and Berlin, 1976), flow cytometry (Szöllösi et al., 1984; Chan et al., 1979; Trón et al., 1984), and FET microscopy (Uster and Pagano, 1986; Herman, 1989). An alternative approach is to directly measure the fluorescence lifetimes of a donor fluorophore first in the absence, and then in the presence of an acceptor molecule (Bunting and

Cathou, 1973). In the latter case, there is an additional de-excitation pathway available to the excited donor molecule, thus decreasing the donor fluorescence lifetime relative to that of donor without acceptor. The efficiency or quantum yield of energy transfer is derived from the two lifetime measurements. Each of the methods mentioned above can be difficult to use quantitatively. Time domain lifetime measurements require that the excitation pulse curve be deconvoluted from the data before analysis. Frequency domain lifetime measurements require complex equipment and their extension to multiexponential decays is mathematically involved. Flow cytometric measurements of sensitized emission require the simultaneous use of two excitation and two or more emission wavelengths and extensive background correction algorithms (Chan et al., 1979). Steady-state spectra also require corrections and are degraded by sample light scattering (Fleming et al., 1979).

Jovin and co-workers (1989a,b, 1990) and Kubitscheck et al. (1991, 1993) have introduced a new and promising FET method which is related to, but more straightforward than, direct lifetime measurements. This method measures photobleaching rates of single cells (or other systems) labeled with donor fluorophores and with donor and acceptor fluorophores. When acceptors are present, photobleaching proceeds more slowly than in their absence. The difference is due to depopulation of the donor excited state by the energy transfer pathway provided by the acceptor. The two photobleaching rates are used to calculate the FET efficiency. Kubitscheck and co-workers have also used this information to evaluate ligand binding constants to membrane proteins (1991) and to assess radial distributions of donor and acceptor sites (1993).

We present practical aspects of the quantitative applications of this photobleaching approach to studies of energy transfer on single cells (Arnette et al., 1990). As a test for the method, we have investigated the differential membrane-binding effects of concanavalin A (Con A) and succinyl concanavalin A (S Con A).

## THEORY

### Kinetic development for simple processes

When a donor molecule D is excited by radiation of intensity $I$ and of wavelength at or near its absorption maximum, an excited donor molecule $D^*$ is created with a first-order rate constant $Ik_e$. $D^*$ may return to its ground state via several pathways, each having different first-order rate constants: fluorescence emission $(k_f)$, various nonradiative pathways $(k_n)$, and, in the presence of an acceptor A, resonant energy transfer $(k_t)$. Also, irreversible photobleaching of $D^*$ may occur with a pseudo-first-order rate constant $k_b$, producing a non-fluorescent chemical species $B$. These pathways are summarized in Eq. 1:

$$D \underset{k_f + k_n + k_t}{\overset{Ik_e}{\rightleftarrows}} D^* \overset{k_b}{\underset{O_2, etc.}{\rightarrow}} B \qquad (1)$$
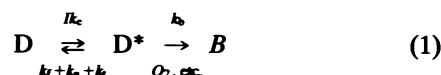
As a cell labeled with D molecules is bleached, a net decrease in the fluorescence intensity $F(t)$ with time is observed. The time derivative of $F(t)$, $F'(t)$, depends on the instantaneous excited donor concentration $[D^*(t)]$, which in turn depends on the number of deactivation pathways available and on their respective rate constants. The presence of the FET pathway decreases $[D^*(t)]$ and so decreases the photobleaching rate $F(t)$. The differences in $F(t)$ with and without the presence of A molecules allow the calculation of the FET efficiency.

We quantify these ideas by solving the differential equations associated with the scheme in Eq. 1:

$$\frac{d}{dt}[D(t)] = -k_e I[D(t)] + (k_n + k_f + k_t)[D^*(t)]$$

$$\frac{d}{dt}[D^*(t)] = k_e I[D(t)] - (k_n + k_f + k_t)[D^*(t)] - k_b[D^*(t)]$$
$$(2)$$

where $I$ is the incident radiation intensity. Note that, within this formalism, the absence of acceptors corresponds to $k_t = 0$.

We assume that $D^*$ obeys the steady-state approximation, so that very shortly after the start of a photobleaching experiment, the change in $D^*$ with time is 0. After applying standard methods (Moore, 1962), the final result is

$$F(t) = \frac{k_e Ik_f}{k_n + k_f + k_t + k_b} \exp\left[-\frac{k_e Ik_b}{k_n + k_f + k_t + k_b}\right] \qquad (3)$$

For a typical donor such as fluorescein isothiocyanate, $k_n$ is about $1.5 \times 10^8 \text{ s}^{-1}$ and $k_f$ is about $1 \times 10^8 \text{ s}^{-1}$ (Cantor and Schimmel, 1980). The excitation rate $k_e I$ is $2303\epsilon I\lambda/hc$ or $0.015 \text{ s}^{-1}$ and apparent bleaching rates $k$ are observed to be

$1 \text{ s}^{-1}$. We can thus estimate $k_b$ as $k(k_n + k_f)/k_e I$ or $170 \text{ s}^{-1}$. Thus $k_b$ is much smaller than any other terms in the denominator of Eq. 3. This permits simplification of the observed signal to

$$F(t) = \frac{k_e Ik_f}{k_n + k_f + k_t} \exp\left[-\frac{k_e Ik_b}{k_n + k_f + k_t}t\right] \qquad (4)$$

The coefficient of $t$ in Eq. 4 is the apparent donor photobleaching rate constant $k$ which changes to reflect energy transfer. It can conveniently be measured from the behavior of the fluorescence signal at time 0:

$$k = F'(0)/F(0) \qquad (5)$$

Once $k_D$ and $k_{DA}$ are obtained from measurements on donor-only and donor-plus-acceptor cells, the fluorescence energy transfer efficiency $E$, i.e., the quantum yield for energy transfer (Lakowicz, 1983), can be evaluated as

$$E = \frac{k_t}{k_n + k_f + k_t}$$
$$= 1 - k_{DA}/k_D \qquad (6)$$

### Multiexponential processes

We observe experimentally, even in the absence of energy transfer, a distribution of apparent photobleaching rate constants. As suggested by Eq. 4, we represent this distribution as a sum of exponentials:

$$F(t) = F(0) \sum \alpha_i \exp(-k_i t) \qquad (7)$$

where $F(0)$ is the initial fluorescence, $\alpha_i$ are the fractional amplitudes of the various decay rates, and $k_i$ are the various apparent photobleaching rates as defined in Eq. 4. We now consider the interpretation of this distribution.

Jongsma et al. (1971) showed that photobleaching of fluorescein isothiocyanate (FITC) solutions gave linear plots of log $F(t)$ vs. $t$. When FITC was conjugated to cell surface proteins, however, these authors found log plots of $F(t)$ vs. $t$ to be strongly curved. Similar variation in photobleaching rates is observed for fluorescent antibody conjugates bound to cell surfaces (Benson et al., 1985). One possible explanation for these findings can be found in Eq. 1. The rate of excited state photobleaching is dependent on various environmental parameters including the availability of oxygen in the vicinity of a $D^*$ molecule. On a protein or cell surface, a variety of chromophore microenvironments may exist, each with a different value of $k_b$. In systems involving energy transfer between randomly located and/or oriented chromophores, heterogeneity in the constant $k_t$ must also be expected. While the other rate constants $k_e$, $k_n$, and $k_f$ are also strictly functions of the environment of the particular donor chromophore, in the measurements performed here, variation in these quantities is expected to be much less than that in $k_b$ and/or $k_t$. We assume here that these quantities have single values for all donor molecules. Given heterogeneity in $k_b$

and/or $k_t$, the observed fluorescence signal becomes

$$F(t) = \sum_{k_t, k_b} n(k_t, k_b) \frac{k_e I k_f}{k_n + k_f + k_t}$$

$$\cdot \exp\left[ -\frac{k_n + k_f}{k_n + k_f + k_t} \frac{k_e I k_b}{k_n + k_f} t \right] \quad (8)$$

where $n(k_t, k_b)$ denotes the fraction of molecules having particular values of $k_t$ and $k_b$.

Eq. 8 is written so as to show that, if heterogeneity in energy transfer rates is small, photobleaching kinetics measured in the presence of acceptor will exhibit the same kinetic heterogeneity as donor-only kinetics but with each individual rate reduced by a constant factor $(k_n + k_f)/(k_n + k_f + k_t)$ reflecting energy transfer. Thus, in such a case, the energy transfer efficiency can satisfactorily be evaluated as in Eq. 6 but using average photobleaching rate constants for donor-only and donor-plus-acceptor cells. Any averaging method will be satisfactory for this use, provided that the same chromophores contribute to the donor-only and donor-plus-acceptor averages. The most appropriate average will depend upon how confidently various rate constants can be determined. Because the measurement of the slower bleaching rates is complicated by various instrumental and sample-related factors, we focus on the faster apparent bleaching rates and employ the number average of the observed $k_i$. This quantity is easily obtained from the results of fitting observed data to Eq. 7.

$$\bar{k} = \sum_i \alpha_i k_i$$

$$= F'(0)/F(0) \quad (9)$$

The apparent FET efficiency $E_{app}$ can then be calculated in analogy with Eq. 6. Provided that variation in $k_b$ is uncorrelated with possible variation in $k_t$, the effect of possible heterogeneity in $k_b$ and $k_t$ on $E_{app}$ is found by combining Eqs. 8–10 and averaging over $k_b$ and $k_t$.

$$E_{app} = 1 - \bar{k}_{DA}/\bar{k}_D \equiv \bar{E} \quad (10)$$

where $\bar{E}$ is the number-average energy transfer efficiency. This calculation shows that variation in $k_b$ is without effect on $E_{app}$. Likewise, $E_{app}$ is independent of the variance $\sigma_E^2$ of the distribution of energy transfer efficiencies.

As noted above, various averages of the rate constants can be suitable if they can satisfactorily be determined experimentally. Jovin and Arndt-Jovin (1989a) effectively evaluate a different quantity $\bar{k}'$, namely

$$\bar{k}' = F(0) \bigg/ \int_0^\infty F(t)\, dt \quad (11)$$

and this quantity is seen to be one over the average reciprocal rate constant or

$$\bar{k}' = \frac{1}{\sum_i \alpha_i (1/k_i)} \quad (12)$$

Thus, the average rate constant we employ reflects most

strongly the faster rate constants of any distribution whereas that used by Jovin and co-workers focuses on the slower rates. One reason motivating our use of $\bar{k}$ is that small amounts of fluorescence signal arising from slowly bleachable sources like cellular autofluorescence have much less impact on the evaluation of $\bar{k}$ than of $\bar{k}'$.

## Data analysis

This development suggests how to measure the rate distributions of interest. In a typical fluorescence microscope photometer, we bleach cells labeled with donor only and with donor plus acceptor on a convenient time scale, usually several seconds. The initial fluorescence intensity $F(0)$ is adjusted via $I$ to the desired order of magnitude, and $I$ is held constant for the two cell groups. Data on individual cells are collected over a time span long enough to insure the accurate determination of photobleaching rates for the majority of chromophores. Data from individual cells can be processed individually or data for several cells within each group can be summed and analyzed as a group for the relevant rate constant distribution. We employ direct multiexponential fitting, wherein the data are least-squares fitted directly to Eq. 7, typically containing three exponentials. The fitting is quickly accomplished using the Marquardt nonlinear algorithm (Bevington, 1969). Since data are obtained by photon counting, individual points are weighted according to Poisson statistics, i.e., by the inverse first power of the calculated fluorescence. Error estimates for the fitted parameters are approximated using the linear estimates normally used with such procedures (Bevington, 1969).

## MATERIALS AND METHODS

### Chemicals

### Cell preparation

Cells were then washed three times with 10 ml balanced salt solution, centrifuging after each wash, and the cells aliquoted in 1 ml samples containing about $1 \times 10^6$ cells/ml each.

The energy transfer efficiency was measured as a function of the ratio A/D of acceptor to donor lectin molecules used to label cells. We required that donor-only and acceptor-plus-donor cell groups be exposed to the same donor and total lectin concentrations and that the total concentration be high enough to saturate plasma membrane glycoproteins. For acceptor-plus-donor labeling solutions, we divided the desired total lectin concentration among donor- and acceptor-labeled lectins according to the desired A/D ratio. For the donor-only samples, an equivalent concentration of unlabeled lectin replaced the acceptor-labeled material. Research with other cell types (Steinkamp and Kraemer, 1974; Eisen et al., 1977; Chan et al., 1979) has shown that a Con A concentration of 50 $\mu$g/ml is sufficient to saturate samples of our cell concentration. Therefore, we used labeling concentrations of 50 $\mu$g/ml for Con A and 25 $\mu$g/ml for succinyl Con A.

Culture tubes were prepared in the dark with labeling solutions formulated as described above. To each tube was added a 1 ml aliquot of the cell suspension prepared as discussed previously. Labeling proceeded for 45 min at 25°C. After labeling, the samples were rinsed of unbound lectin by washing three times with balanced salt solution, then resuspended in 0.2 ml balanced salt solution and stored at 25°C.

## Photobleaching rate constant measurements

Measurements were made both with a fluorescence microscope photometer described previously (Leuther et al., 1981) and with a new system. The new microscope photometer shown in Fig. 1 is based on an inverted-configuration Zeiss Axiomat microscope equipped with a fluorescence vertical illuminator, photometer module, thermoelectrically controlled thermal stage, and scanning stage. Fluorescence isolated by the photometer module is conducted by 3-mm glass fiberoptic bundles to a Hamamatsu R943 photomultiplier tube mounted in a thermoelectrically cooled housing. Fluorescence excitation is provided by a Coherent Radiation Innova 100 argon ion laser operating under light control at 488 nm. The intensity of the laser radiation focused on the cell is 2.5–5 mW and this quantity is held constant between measurements on donor-only and donor-plus-acceptor cells. The $1/e^2$ Gaussian spot diameter was 18 $\mu$m. Fluorescence intensity measure-

ments were obtained via photon counting using a Princeton Applied Research 1182 amplifier/discriminator. Intensities are expressed as counts per second (cps). Donor fluorescence was isolated with a standard fluorescein filter set together with a short pass fluorescein-selective filter to remove red tetramethylrhodamine fluorescence. This combination was highly effective in rejecting TRITC fluorescence, since cells labeled with TRITC-Con A only gave green fluorescence signals indistinguishable from completely unlabeled cells. Neither cell autofluorescence nor TRITC fluorescence contributes appreciably to rate constant determinations. Fluorescein is quite easily photobleached and the bleaching rates of autofluorescence and of TRITC fluorescence are only 9% and 7% of this FITC bleaching rate, respectively. Because of the manner in which A is calculated, weak fluorescence signals from such slowly bleached species have negligible effects on measured energy transfer efficiencies.

Single cells were identified and centered in the microscope field. At time 0, an electronically controlled shutter was opened to allow laser radiation to impinge on the cell. Simultaneously, a computer program was activated to record the output of the photomultiplier measuring cellular fluorescence. Data were collected at 0.01-s intervals for a minimum of 2.5 s. Typically, about 20 cells from each sample were photobleached in this manner. Traces showing unusual noise or cell movement were discarded, and the remaining data, always at least 10 cells, were analyzed individually and/or summed pointwise to give a composite curve for analysis.

## Cytometric energy transfer measurements on lectin-labeled cells

Cell samples, prepared as previously described, were examined using an EPICS 752 flow cytometer (Coulter Instruments, Hialeah, FL) to measure resonant energy transfer between donor (FITC)-labeled and acceptor (TRITC)-labeled Con A bound to B lymphocytes. Dual wavelength (488 and 575 nm) excitation was used to evaluate energy transfer efficiency in labeled cells. Three intensity histograms of 20,000 cells were recorded for each cell sample: 488 nm excitation and 525 nm emission, 488 nm excitation and >590 nm emission and 575 nm excitation and >590 nm emission. Fluorescence energy transfer was calculated from quenching of 525 nm



FIGURE 1 Microscope photometer for use in single cell fluorescence energy transfer, fluorescence photobleaching recovery, and digital video microscopic measurements. The functions of the various components are described in the text.
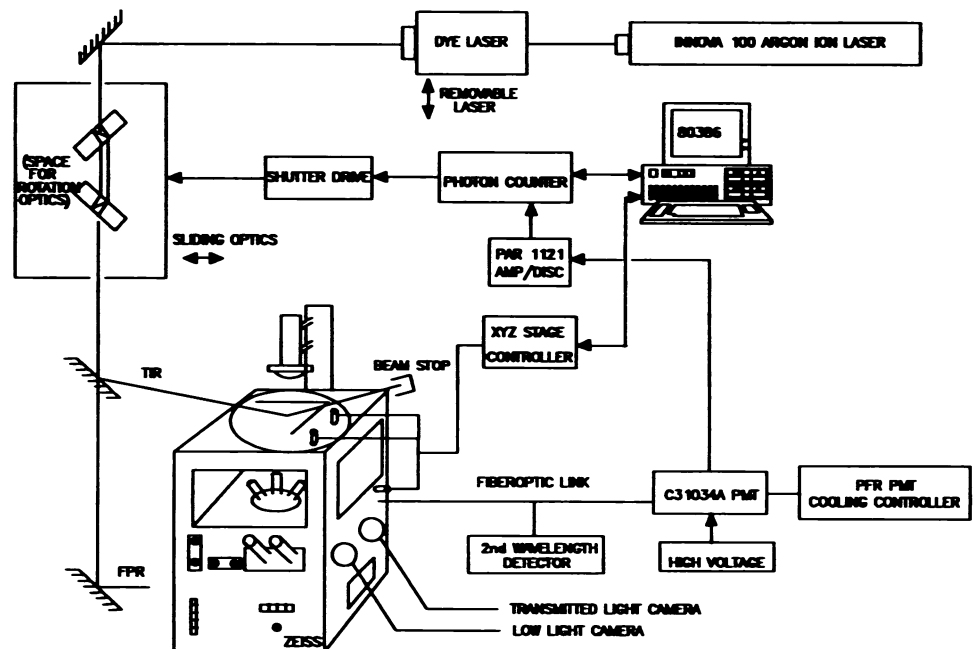
donor fluorescence upon 488 nm excitation (Stryer, 1978). Other measurements were used to verify equal binding affinities of donor- and acceptor-labeled lectins.

## RESULTS AND DISCUSSION

### Photobleaching kinetic results

When viewed in the microscope, the cells were ring-stained and showed no signs of capping. Cells treated with Con A were highly agglutinated, and these clusters were avoided to exclude possible intercellular energy transfer. Cells treated with succinyl Con A were almost completely unassociated, as would be expected. For labeled cells, initial fluorescences typically exceeded 100,000 cps. Unlabeled cells showed quite low autofluorescence, usually about 4000 cps. The photobleaching decay kinetics of two individual cells, one labeled with FITC-Con A only and the other with TRITC-Con A and FITC-Con A in a 3:1 molar ratio are shown in Fig. 2. The kinetic parameters obtained from fitting these data to a three-exponential decay model are shown in Table 1. It is clear by inspection that three exponentials are required to give a satisfactory fit. Moreover, this same model is sufficient to fit the data fully since the values of reduced $\chi^2$ for such fits average ~1.0. The statistical uncertainty in individual average photobleaching rate constants was variable; but, for example, over 16 FITC-only cells this uncertainty averaged 5.2%.

The distribution of average photobleaching rate constants for these two cell groups is shown in Fig. 3. The upper and lower panels show rate constant histograms for 16 donor-only cells and 20 donor-plus-acceptor cells, respectively. The reduction in average rate constants caused by the presence of acceptor is clear. The average rate constant for the donor-only group is 0.40 s$^{-1}$, while that for the donor-plus-acceptor cells is 0.21 s$^{-1}$ implying, via Eq. 15, a mean energy transfer

**TABLE 1   Results of least-squares analysis of photobleaching traces for two individual B lymphocytes labeled with FITC-Con A only and with a 3:1 molar ratio of TRITC- and FITC-Con A\***

| Parameter | FITC-Con A | TRITC- and FITC-Con A |
|---|---|---|
| Initial fluorescence | 1.196 × 10⁶ cps | 0.462 × 10⁶ cps |
| 1st lifetime | 0.62 ± 0.04 s | 0.89 ± 0.05 s |
| 1st fractional amplitude | 0.18 ± 0.01 | 0.12 ± 0.01 |
| 2nd lifetime | 5.1 ± 0.2 s | 6.7 ± 0.06 s |
| 2nd fractional amplitude | 0.35 ± 0.01 | 0.37 ± 0.01 |
| 3rd lifetime | 30.4 ± 0.5 s | 70.7 ± 0.05 s |
| 3rd fractional amplitude | 0.47 ± 0.1 | 0.51 ± 0.01 |
| Average rate constant | 0.39 ± 0.02 s$^{-1}$ | 0.20 ± 0.01 s$^{-1}$ |
| Reduced $\chi^2$ | 1.02 | 0.90 |

\* The raw data used in the fitting procedure are shown as points in Fig. 2, *left*. The smooth curves shown in that figure are calculated from the above numbers.

efficiency of 48%. The standard deviations of both *groups* of rate constants are equal at about 0.04 s$^{-1}$, or about 10% and 20% for donor-only and donor-plus-acceptor cell groups, respectively. The standard deviations of the *mean* rate constants are about 0.01 s$^{-1}$, or about 2% and 5% for donor-only and donor-plus-acceptor cell groups, respectively. Propagation of errors suggests that energy transfer efficiencies calculated from such data should have a standard deviation of perhaps 6%. It also appears that the variation of rate constants among cells of each group substantially exceeds the statistical uncertainty in an individual rate constant determination. One concludes that there is considerable real variation in bleaching rates between cells and that it is advantageous to evaluate these rates on a cell-by-cell basis so that this variation can be delineated. Nonetheless, it is possible to sum data collected from a number of individual cells and to analyze the single summed data set. Numerically, the results of such
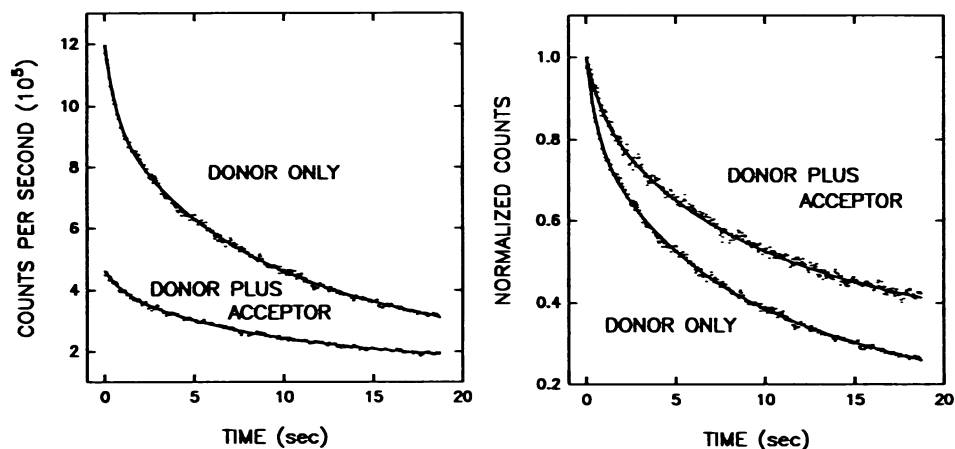


FIGURE 2   Typical experimental data obtained from single murine B lymphocyte photobleaching curves. The donor-only cell was labeled with unconjugated Con A and FITC-Con A at a molar ratio of 3:1 and a total lectin concentration of 25 µg/ml as described in the text. The donor-plus-acceptor cell was labeled with FITC-Con A and TRITC-Con A at a molar ratio of 3:1 and a total lectin concentration of 25 µg/ml. Temperature 25°C, laser power 2.5 mW, and spot diameter 18 µm. The *left* trace shows raw data points and fitted curves obtained from three-exponential fits, the numerical results of which are shown in Table 1. The *right* trace shows the same data normalized to the initial intensities so that the reduction in photobleaching rate caused by the introduction of acceptor can more clearly be seen.
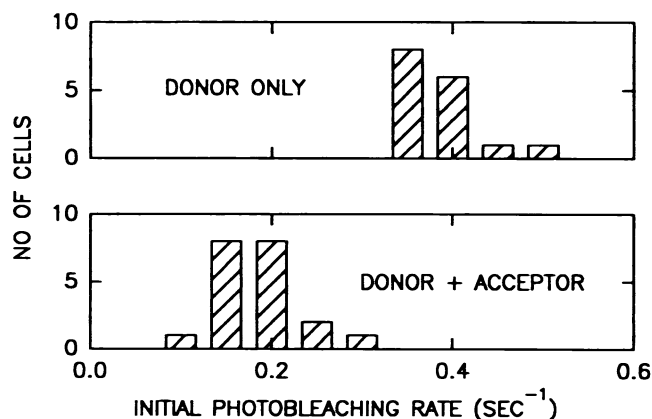
FIGURE 3   Histograms of average rate constant distributions for 16 donor-only (top) and 20 donor-plus-acceptor cells (bottom) labeled as described in Figure 1. The shift in the rate constant distribution caused by the introduction of acceptor is apparent from comparison of the two panels.

**TABLE 2   Average photobleaching rate constants and fluorescence energy transfer efficiencies as functions of A/D ratios for Con A bound to murine B lymphocytes[*]**

| A/D[‡] | $k_D$ (s⁻¹)[§] | $k_{DA}$ (s⁻¹)[¶] | $E$[∥] | $E$[**] |
|---|---|---|---|---|
| 0.33 | 0.63 ± .01 | 0.59 ± .01 | 0.03 ± .03 | n.d. |
| 0.54 | 0.67 ± .01 | 0.67 ± .01 | −0.01 ± .02 | n.d. |
| 1.00 | 1.00 ± .01 | 0.67 ± .01 | 0.32 ± .02 | 0.35 ± 0.03 |
| 1.67 | 0.67 ± .01 | 0.42 ± .01 | 0.37 ± .02 | n.d. |
| 3.00 | 0.40 ± .01 | 0.21 ± .01 | 0.48 ± .02 | 0.54 ± 0.03 |
| 4.00 | 0.40 ± .01 | 0.20 ± .01 | 0.49 ± .02 | n.d. |

\* Temperature 25°C, laser power 2.5–5.0 mW, spot diameter 18 μm.
‡ A/D molar ratio.
§ Average photobleaching rate constant for cells labeled with FITC-con A only.
¶ Average photobleaching rate constant for cells labeled with the indicated molar ratio of TRITC-Con A and FITC-Con A.
∥ Energy transfer efficiency, calculated from photobleaching data according to Eq. 10.
\** Energy transfer efficiency, calculated from flow cytometric measurements of donor quenching according to method of Stryer (1978).

summed fitting are identical to those obtained by averaging individual cell results (data not shown).

The possible effects of bleaching power levels on measured energy transfer were explored in a separate measurement of energy transfer between B cell-bound Con A molecules at an A/D ratio of 3:1. Bleaching powers of 6, 12, and 30 mW yielded energy transfer efficiencies of 0.30, 0.29, and 0.30, respectively. Thus we conclude that energy transfer efficiencies are grossly independent of bleaching power as one would expect.

In summary, it appears that energy transfer efficiencies can be measured by photobleaching methods with a statistical uncertainty of perhaps 2% for energy transfer efficiencies near 50%. Most of this uncertainty arises from variation between cells. Because the cells studied here are a heterogeneous population of primary cultured cells labeled with a lectin of rather broad specificity, this uncertainty in energy transfer efficiencies is almost certainly a maximum estimate and should be appreciably lower for a homogeneous cell population labeled with a monospecific immunochemical. The question arises as to how well these results accord with energy transfer efficiencies measured by more conventional methods. Flow cytometry was used to measure quenching of FITC-Con A donor fluorescence by TRITC-Con A acceptor in cells samples prepared like those used in photobleaching measurements. These results are presented in Table 2 and show excellent agreement between the energy transfer efficiencies obtained by the two methods. In fact, there is less variation among cells in average rate constants (see, for example, Fig. 3) than in cytometrically measured fluorescence intensities of labeled cell populations where coefficients of variation of 100% are not uncommon. This points up a fundamental advantage of kinetic-based over intensity-based methods.

Although we have not used continuous rate distributions to analyze energy transfer data, these distributions illustrate how photobleaching rate constant distributions change in the presence of acceptor chromophores. Exponential sampling (Ostrowski et al., 1981) assumes that $F(t)$ contains a con-

tinuum of photobleaching rate constants and therefore is relatively model-independent. The decay curve is inverted via a discrete analogue of the Laplace transform to give a numerical approximation of a continuous rate constant distribution. Comparison of rate constant distributions for donor-only cells and for donor-plus-acceptor cells (data not shown) shows that the addition of acceptors shifts the rate distribution to the left, i.e., to slower rates as expected. The distributions have two or three major modes, followed by a continuum at very slow rates. These qualitative features agree well with those observed by Benson et al. (1985).

## Inter-lectin energy transfer

The measured photobleaching rates and calculated energy transfer efficiencies for both Con A- and succinyl Con A-labeled cells are summarized in Tables 2 and 3, respectively, and energy transfer efficiencies are plotted versus A/D ratios in Fig. 4. Transfer efficiency rises rapidly with increasing A/D ratio and plateau at about 3 for both lectins. There are no published fluorescence energy transfer studies

**TABLE 3   Average photobleaching rate constants and fluorescence energy transfer efficiencies as functions of A/D ratio for succinyl Con A bound to murine B lymphocytes[*]**

| A/D[‡] | $k_D$ (s⁻¹)[§] | $k_{DA}$ (s⁻¹)[¶] | $E$[∥] |
|---|---|---|---|
| 0.33 | 0.56 ± .01 | 0.56 ± .01 | −0.01 ± .03 |
| 1.00 | 0.67 ± .01 | 0.53 ± .01 | 0.24 ± .02 |
| 1.67 | 0.71 ± .01 | 0.50 ± .01 | 0.29 ± .02 |
| 3.00 | 0.54 ± .01 | 0.37 ± .01 | 0.32 ± .02 |
| 4.70 | 0.54 ± .01 | 0.35 ± .01 | 0.36 ± .02 |

\* Temperature 25°C, laser power 2.5–5.0 mW, spot diameter 18 μm.
‡ A/D molar ratio.
§ Average photobleaching rate constant for cells labeled with FITC-succinyl Con A only.
¶ Average photobleaching rate constant for cells labeled with the indicated molar ratio of TRITC-succinyl Con A and FITC-succinyl Con A.
∥ Energy transfer efficiency, calculated from photobleaching data according to Eq. 10.

FIGURE 4 Energy transfer efficiency E as a function of A/D ratio for lectins Con A (○) succinyl Con A (●) bound to murine B lymphocytes 25°C, laser power 2.5 mW, and spot diameter 18 μm.



ACCEPTOR TO DONOR RATIO (A/D)
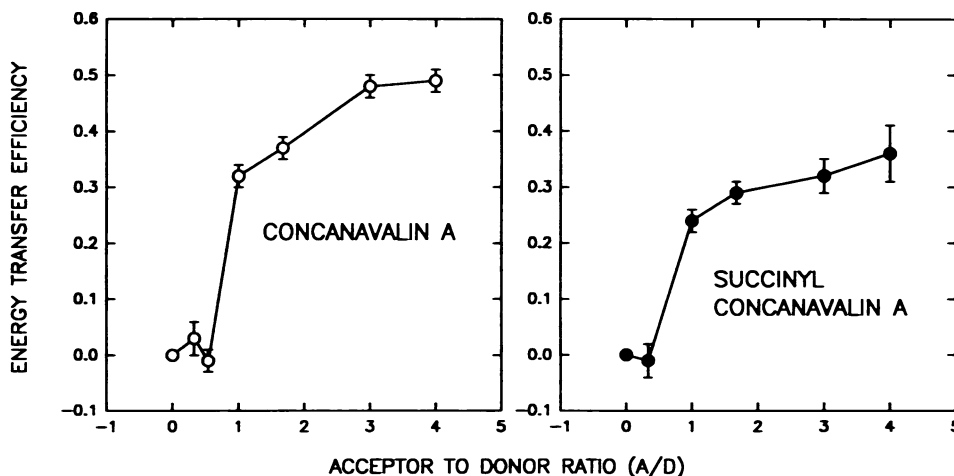
on Con A and murine B lymphocytes with which we can compare our results. There are, however, such studies with Con A on other cell types. Since Con A "receptors" are glycoproteins of a nonspecific and ubiquitous nature, it is reasonable to compare our results with those of such other studies. Our maximum observed transfer efficiency was 0.49 at A/D = 4. Fernandez and Berlin (1976) investigated murine 3T3 fibroblasts via steady-state fluorescence spectroscopy and found a maximum efficiency of 0.49 at A/D = 5. Using a flow cytometric method, Szöllösi et al. (1984) found a maximum efficiency of 0.35 at A/D = 4.3 for HK22 murine lymphoma cells. Chan et al. (1979) found a transfer efficiency of 0.57 for transformed Friend erythroleukemia cells by flow cytometry. These various values are in excellent agreement with our work, especially considering that three different cell types are involved. The only report in the literature concerning energy transfer with succinyl Con A is a qualitative spectroscopic study by Steiner (1984). This author does not calculate efficiencies, but does observe fluorescence energy transfer with succinyl Con A bound to platelets. The effect is maximized at A/D = 3.0 and decreases on either side of this value, thus displaying a true maximum. This is different from the previously quoted Con A studies, wherein the maximum energy transfer efficiency occurred at the highest A/D values reported.

It is evident from Fig. 4 that energy transfer between cell-bound succinyl Con A molecules is almost as efficient as between cell-bound molecules of intact Con A. This could arise from three situations. First, most membrane glycoproteins could be present in virtually closest packed protein arrays in the membrane. Second, multiple lectin molecules could bind to different glycosylation sites on the same protein. Alternatively, succinyl Con A could be almost as efficient as intact Con A in cross-linking surface glycoproteins. This appears likely, since membrane proteins labeled with succinyl Con A generally seem to be rotationally immobile, suggesting cross-linking into large aggregates. This would require that succinyl Con A be *functionally* divalent, as its dimeric structure could well permit.

Our technique differs in its application that of Jovin and Arndt-Jovin (1989a). These authors employ a time integral

of the fluorescence intensity as a measure of the total number of fluorophores. This necessitates following the photobleaching curve to its baseline. As stated earlier, there is essentially a continuum of photobleaching rate constants, some of which are very small. This method is thus potentially subject to errors due to the difficulty of accurately measuring these small rate constants. Our technique avoids this problem by focusing on the faster rate constants in the distribution, quantities which are easily and accurately measured.

Photobleaching FET techniques offers advantages over other methods of FET measurement. First, being kinetic techniques, photobleaching methods are insensitive to the absolute signal levels detected. Second, these methods are conveniently applied to individual cells. Cells can be selected individually and cell clusters or nonviable cells can be avoided. A third attraction is the requirement for only simple and inexpensive instrumentation, namely a low-powered argon laser and a microscope photometer. Finally, particularly in comparison with methods involving donor emission, photobleaching measurements require collection of fewer types of data, so that data analysis is easily performed on-line.

## REFERENCES

Arnette, J. K., K. A. Reedquist, D. A. Roess, and B. G. Barisas. 1990. FET measurement of interprotein distances in membrane protein aggregates on single cells. *Biophys. J.* 57:252a.

Benson, D. M., J. Bryan, A. L. Plant, A. M. Grotto, Jr., and L. C. Smith. 1985. Digital imaging fluorescence microscopy: spatial heterogeneity of photobleaching rate constants in individual cells. *J. Cell Biol.* 100:1309–1323.

Bevington, P. R. 1969. Data Reduction and Error Analysis for the Physical Sciences. McGraw-Hill, New York.

Bunting, J. R., and R. E Cathou. 1973. Energy transfer distance measurements in immunoglobulins. II. Localization of the hapten binding sites and the interheavy chain disulfide bond in rabbit antibody. *J. Mol. Biol.* 77:223–235.

Cantor, C. R., and P. R. Schimmel. 1980. Biophysical Chemistry II, Techniques for the Study of Biological Structure and Function. W. H. Freeman, San Francisco. 446.

Chan, S. S., D. J. Arndt-Jovin, and T. M. Jovin. 1979. Proximity of lectin receptors on the cell surface measured by fluorescence energy transfer in a flow system. J. Histochem. Cytochem. 27:56–64.

Eisen, H., S. Nasi, C. P. Georgopoulos, D. Arndt-Jovin, and W. Ostertag. 1977. Surface changes in differentiating friend erythroleukemic cells in culture. Cell. 10:689–695.

Fairclough, R. H., and C. R. Cantor. 1978. The use of singlet-singlet energy transfer to study macromolecular assemblies. Methods Enzymol. 48:347–379.

Fernandez, S. M., and R. D. Berlin. 1976. Cell surface distribution of lectin receptors determined by resonance energy transfer. Nature. 264:411–415.

Fleming, P. J., D. E. Koppel, A. L. Y. Lau, and P. Strittmatter. 1979. Intramembrane position of the fluorescent tryptophanyl residue in membrane-bound cytochrome $b_5$. Biochemistry. 18:5458–5464.

Fung, B. K., and L. Stryer. 1978. Surface density determination in membranes by fluorescence energy transfer. Biochemistry. 17:5241–5248.

Herman, B. 1989. Resonance energy transfer microscopy. Methods Cell Biol. 30:219–243.

Jongsma, A. P. M., W. Hijmans, and J. S. Ploem. 1971. Standardization and calibration in microfluorometry. Histochemie. 25:329–345.

Jovin, T. M., and D. J. Arndt-Jovin. 1989a. FRTE microscopy: digital imaging of fluorescence resonance energy transfer. Applications in cell biology. In Cell Structure and Function by Microspectrofluorometry. E. Kohen, J. G. Hirschberg, and J. S. Ploem, editors. Academic Press, New York. 99–117.

Jovin, T. M., and D. J. Arndt-Jovin. 1989b. Luminescence digital imaging microscopy. Annu. Rev. Biophys. Biophys. Chem. 18:271–308.

Jovin, T. M., D. J. Arndt-Jovin, G. Marriott, R. M. Clegg, M. Robert-Nicoud, and T. Schormann. 1990. Distance wavelength and time: the versatile 3rd dimensions in light microscopy. In Optical Microscopy for Biology. Wiley-Liss, New York. 575–602.

Kubitscheck, U., M. Kircheis, R. Schweitzer-Stenner, M. Derybrodt, T. M. Jovin, and I. Pecht. 1991. Fluorescence resonant energy transfer on single

living cells: application to binding of monovalent haptens to cell-bound immunoglobulin E. Biophys. J. 60:307–318.

Kubitscheck, U., R. Schweitzer-Stenner, D. Arndt-Jovin, T. M. Jovin, and I. Pecht. 1993. Distribution of type I Fcε-receptors on the surface of mast cells probed by fluorescence resonance energy transfer. Biophys. J. 64:110–120.

Lakowicz, J. K. 1983. Principles of Fluorescence Spectroscopy. Plenum Press, New York. 306.

Leuther, M. D., J. S. Peacock, H. Krakauer, and B. G. Barisas. 1981. Changes in lectin receptor lateral mobilities accompany lymphocyte stimulation. J. Immunol. 127:893–899.

Moore, W. J. 1962. Physical Chemistry. Prentice-Hall, Englewood Cliffs, NJ. 279.

Ostrowski, N., D. Sornette, P. Parker, and E. R. Pike. 1981. Exponential sampling method for light scattering polydispersity analysis. Optica Acta. 28:1059–1070.

Steiner, M. 1984. Changes in the distribution of platelet membrane proteins revealed by energy transfer. Biochim. Biophys. Acta. 805:53–58.

Steinkamp, J. A., and P. M. Kraemer. 1974. Flow microfluorometric studies of lectin binding to mammalian cells. II. Estimation of the surface density of receptor sites by multiparameter analysis. J. Cell Physiol. 84:197–204.

Stryer, L. 1978. Fluorescence energy transfer as a spectroscopic ruler. Annu. Rev. Biochem. 47:819–846.

Szöllösi, J. L. Trón, S. Damjanovich, S. H. Helliwell, D. Arndt-Jovin, and T. M. Jovin, T. M. 1984. Fluorescence energy transfer measurements on cell surfaces: a critical comparison of steady-state fluorometric and flow cytometric methods. Cytometry. 5:210–216.

Trón, L., J. Szöllösi, S. Damjanovich, S. H. Helliwell, D. Arndt-Jovin, and T. M. Jovin. 1984. Flow cytometric measurement of fluorescence resonance energy transfer on cell surfaces. Quantitative evaluation of the transfer efficiency on a cell-by-cell basis. Biophys. J. 45:939–946.

Uster, P. S., and R. E. Pagano, R. E. 1986. Resonance energy transfer microscopy: observations of membrane-bound fluorescent probes in model membranes and in living cells. J. Cell Biol. 103:1221–1234.